Thermal radition effect on flow and heat transfer of unsteady MHD micropolar fluid over vertical heated non-isothermal stretching surface using group analysis

Article *in* Applied Mathematics and Mechanics · June 2013

DOI: 10.1007/s10483-013-1701-6

Appl. Math. Mech. -Engl. Ed., **34**(6), 703–720 (2013)
DOI 10.1007/s10483-013-1701-6

Applied Mathematics and Mechanics (English Edition)

Thermal radiation effect on flow and heat transfer of unsteady MHD micropolar fluid over vertical heated nonisothermal stretching surface using group analysis*

I. A. HASSANIEN[1], H. M. EL-HAWARY[1], M. A. A. MAHMOUD[2], R. G. ABDEL-RAHMAN[2], A. S. ELFESHAWEY[2]

(1. Department of Mathematics, Faculty of Science, Assuit University, Assuit 71516, Egypt;
2. Department of Mathematics, Faculty of Science, Benha University, Benha 13518, Egypt)

Abstract The aim of this paper is to study the thermal radiation effects on the flow and heat transfer of an unsteady magnetohydrodynamic (MHD) micropolar fluid over a vertical heated nonisothermal stretching surface in the presence of a strong nonuniform magnetic field. The symmetries of the governing partial differential equations are determined by the two-parameter group method. One of the resulting systems of reduced nonlinear ordinary differential equations are solved numerically by the Chebyshev spectral method. The effects of various parameters on the velocity, the angular velocity, and the temperature profiles as well as the skin-friction coefficient, the wall couple stress coefficient, and the Nusselt number are studied.

Key words thermal radiation, micropolar fluid, unsteady flow, group theoretic method, Chebyshev spectral method

Chinese Library Classification O361.3, O357.3, O357.4
2010 Mathematics Subject Classification 76W05, 76D10, 65L10, 34C14

Nomenclature

B,	applied magnetic field;	I,	dimensionless angular velocity;
T_{c},	characteristic temperature;	ξ,	ratio of the gyration vector component to the fluid shear at a solid boundary;
C_{f},	skin-friction coefficient;		
t,	time;	j,	microinertia density;
c_p,	specific heat at constant pressure;	K,	material parameter;
U_0,	characteristic velocity;	β,	thermal expansion coefficient;
$e_{b\lambda}$,	Plank's function;	K_λ,	absorption coefficient;
u, v,	velocities along the x- and y-axes;	κ,	thermal conductivity;
Re,	Reynolds number;	L,	characteristic length;
r,	radiation parameter;	ν,	kinematic viscosity;
Pr,	Prandtl number;	M,	magnetic parameter;
T,	dimensional temperature;	ρ,	fluid density;
f,	dimensionless stream function;	m_{w},	wall couple stress;
(x, y),	Cartesian coordinate;	γ_0,	spin gradient viscosity;
g,	gravitational acceleration;	m_0,	microrotation parameter;

* Received May 21, 2012 / Revised Jan. 12, 2013
Corresponding author A. S. ELFESHAWEY, Ph. D., E-mail: abeer_elfeshawey@yahoo.com

μ,	dynamic viscosity;	θ,	dimensionless temperature;
N,	angular velocity;	q_{r},	thermal radiation flux;
α,	thermal diffusivity;	ψ,	stream function;
Nu,	Nusselt number;	k,	vortex viscosity.

Scripts

$'$,	differentiation with respect to η;	∞,	free stream condition.
w,	wall condition;		

1 Introduction

Due to the importance in many technological applications such as cooling of nuclear reactors during emergency shutdown, extruding a polymer sheet, stuffing food, cooling electronic devices, enhancing oil recovery, continuously casting, and producing glass fiber, the theory of micropolar fluids has received great attention during recent years[1–3]. Eringen[4–6] was the first author who introduced the concept of a micropolar fluid whose behavior cannot be described by the classical Navier-Stokes theory because of the involving of the effects of two new variables describing the distributions of atoms and molecules inside the fluid elements, i.e., spin and micro inertia. Physically, he represented fluids consisting of randomly oriented particles suspended in a viscous medium. Such fluids have been shown to be able to accurately simulate the flow characteristics of polymeric additives, geomorphological sediments, colloidal suspensions, haematological suspensions, liquid crystals, lubricants, etc. in the context of chemical engineering, aerospace engineering, and industrial manufacturing processes.

Several attempts have concerned with the problems of unsteady micropolar fluids where time is the third independent variable. Agarwal and Dhanapal[7] studied the problem of the unsteady flow and heat transfer for an incompressible micropolar fluid flows over an semi-infinite flat plate, and solved the governing partial differential equations numerically by the finite difference method. Damesh et al.[8] presented the problem of the laminar free convection boundary layer flow of an unsteady micropolar fluid above a heated vertical plate with the prescribed wall heat flux, and solved the governing equations by a finite difference technique. Nazar et al.[9] examined the problem of the flow of a micropolar fluid over a stretching surface. Nazar et al.[10] extended the previous problem of the flow and heat transfer of a micropolar fluid over a nonisothermal stretching surface, and solved the transformed equation numerically by the Keller-box method. Bachok et al.[11] investigated the problem of an unsteady, laminar flow of an incompressible micropolar fluid over a stretching sheet, where the stretching velocity and the surface temperature are functions of the distance and the time.

The mathematical analysis used in the present analysis is the two-parameter group transformation, which leads to a similarity representation of the problem. Some attempts are made to use the group theoretic analysis to find a similarity representation of the problem of flow and heat transfer for micropolar fluids. Ibrahim and Hamad[12] presented similarity solutions for the unsteady mixed convection boundary-layer flow of a micropolar fluid near a stagnation point on a horizontal cylinder. Abd-Elaziz and Ahmed[13] considered the unsteady boundary layer flow of a micropolar fluid near the rear stagnation point of a plane surface in a porous medium. Hassanien and Hamad[14] analyzed the unsteady free convection boundary layer flow of a micropolar fluid on a vertical plate in a thermally stratified medium.

In the above-mentioned studies, the effect of the magnetic field has not been taken into consideration although it has several important applications in many engineering problems such as magnetohydrodynamic (MHD) generators, plasma studies, nuclear reactors, oil exploration, geothermal energy extractions, and boundary layer control in the field of aero-dynamics. Radiation has many industrial applications such as glass production and furnace design and space technology applications such as cosmical flight aerodynamic rockets, propulsion systems, and plasma physics. The considered fluid is taken to be nongray. Then, for an optically thin limit, the fluid does not absorb its own emitted radiation, but absorbs the radiation emitted by the boundaries. Therefore, in the optically thin limit for a gray-gas near equilibrium, the following relation holds[15]:

$$\frac{\mathrm{d}q_{\mathrm{r}}}{\mathrm{d}y} = 4\Gamma(T - T_{\mathrm{w}}), \tag{1}$$

$$\Gamma = \int_0^{\infty} K_{\lambda\mathrm{w}} \Big(\frac{\partial e_{b\lambda}}{\partial T}\Big)_{\mathrm{w}} \mathrm{d}\lambda. \tag{2}$$

The aim of this work is to study the effects of thermal radiation on an MHD unsteady micropolar fluid flow over a nonisothermal vertical stretching surface.

2 Formulation of problem

Consider an unsteady, two-dimensional MHD laminar convective flow of an incompressible, viscous, and micropolar fluid with thermal radiation on a stretching vertical surface. The x-axis is taken along the direction of motion, and the y-axis is taken normal to the surface. It is assumed that a nonuniform magnetic field $B(x)$ is applied in the y-direction. The magnetic Reynolds number of the flow is taken to be small enough so that the induced magnetic field can be assumed to be negligible. The surface temperature is taken as a function of the distance and the time $T_{\mathrm{w}}(x, t)$, while the ambient fluid has a uniform temperature T_∞ which is smaller than $T_{\mathrm{w}}(x, t)$. The gravitational acceleration g acts in the downward direction. The physical model and coordinate system are shown in Fig. 1.

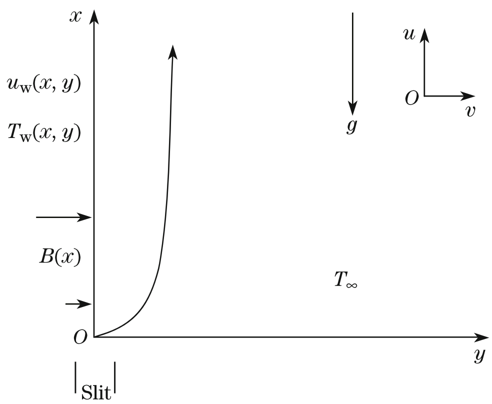

Fig. 1 Physical model and system

The governing equations of the continuity, momentum, and energy for the unsteady flow can be written as follows[15]:

$$\frac{\partial \bar{u}}{\partial \bar{x}} + \frac{\partial \bar{v}}{\partial \bar{y}} = 0, \tag{3}$$

$$\frac{\partial \bar{u}}{\partial \bar{t}} + \bar{u}\frac{\partial \bar{u}}{\partial \bar{x}} + \bar{v}\frac{\partial \bar{u}}{\partial \bar{y}} = \Big(\frac{\mu + k}{\rho}\Big)\frac{\partial^2 \bar{u}}{\partial \bar{y}^2} + g\beta(\overline{T} - \overline{T}_\infty) + \frac{k}{\rho}\frac{\partial \overline{N}}{\partial \bar{y}} - \frac{\sigma B^2(\bar{x})}{\rho}\bar{u}, \tag{4}$$

$$\rho j\Big(\frac{\partial \overline{N}}{\partial \bar{t}} + \bar{u}\frac{\partial \overline{N}}{\partial \bar{x}} + \bar{v}\frac{\partial \overline{N}}{\partial \bar{y}}\Big) = \gamma_0 \frac{\partial^2 \overline{N}}{\partial \bar{y}^2} - k\Big(2\overline{N} + \frac{\partial \overline{N}}{\partial \bar{y}}\Big), \tag{5}$$

$$\frac{\partial \bar{j}}{\partial \bar{t}}+\bar{u}\frac{\partial \bar{j}}{\partial \bar{x}}+\bar{v}\frac{\partial \bar{j}}{\partial \bar{y}}=0, \tag{6}$$

$$\frac{\partial \overline{T}}{\partial \bar{t}}+\bar{u}\frac{\partial \overline{T}}{\partial \bar{x}}+\bar{v}\frac{\partial \overline{T}}{\partial \bar{y}}=\alpha\frac{\partial^2 \overline{T}}{\partial \bar{y}^2}-\frac{1}{\rho c_p}\frac{\mathrm{d}q_{\mathrm{r}}}{\mathrm{d}y} \tag{7}$$

subjected to the boundary conditions

$$\begin{cases} \bar{t}<0: \ \bar{u}=0, \quad \bar{v}=0, \quad \overline{N}=0, \\ \bar{t}>0: \ \bar{u}=\bar{u}_{\mathrm{w}}(\bar{x},\bar{t}), \quad \bar{v}=0, \quad \overline{N}=-\xi\dfrac{\partial \bar{u}}{\partial \bar{y}}, \quad \overline{T}=\overline{T}_{\mathrm{w}}(\bar{x},\bar{t}), \quad j=0 \quad \text{as} \quad \bar{y}=0; \\ \qquad\quad \bar{u}=0, \quad \overline{T}=\overline{T}_{\infty}, \quad \overline{N}=0 \quad \text{as} \quad \bar{y}\to\infty, \end{cases} \tag{8}$$

Assume that the spin gradient viscosity γ_0 is given by

$$\gamma_0=\Big(\mu+\frac{k}{2}\Big)j, \tag{9}$$

where $j=\frac{\nu L}{U_0}$ is the reference length. We now introduce the dimensionless variables as follows:

$$\begin{cases} x=\dfrac{\bar{x}}{L}, \quad y=\dfrac{\bar{y}}{L}\sqrt{Re}, \quad t=\dfrac{\bar{t}U_0}{L}, \quad u=\dfrac{\bar{u}}{U_0}, \\ u_{\mathrm{w}}(x,t)=\dfrac{\bar{u}_{\mathrm{w}}(\bar{x},\bar{t})}{U_0}, \quad v=\dfrac{\bar{v}}{U_0}\sqrt{Re}, \\ T-T_{\infty}=\dfrac{Lg\beta(\overline{T}-\overline{T}_{\infty})}{U_0^2}, \quad T-T_{\mathrm{w}}=\dfrac{Lg\beta(\overline{T}-\overline{T}_{\mathrm{w}})}{U_0^2}, \\ \theta=\dfrac{T-T_{\infty}}{T_{\mathrm{w}}(x,t)-T_{\infty}}, \quad U_0=(Lg\beta T_{\mathrm{c}})^{\frac{1}{2}}, \quad N=\dfrac{L}{U_0\sqrt{Re}}\overline{N}. \end{cases} \tag{10}$$

Introduce the stream function ψ as follows:

$$u=\frac{\partial \psi}{\partial y}, \quad v=-\frac{\partial \psi}{\partial x}. \tag{11}$$

Then, from Eqs. (1)–(8), there are

$$\frac{\partial^2 \psi}{\partial y \partial t}+\frac{\partial \psi}{\partial y}\frac{\partial^2 \psi}{\partial x \partial y}-\frac{\partial \psi}{\partial x}\frac{\partial^2 \psi}{\partial y^2}-(1+K)\frac{\partial^3 \psi}{\partial y^3}-T_1\theta-K\frac{\partial N}{\partial y}+M^*B^2(x)\frac{\partial \psi}{\partial y}=0, \tag{12}$$

$$\frac{\partial N}{\partial t}+\frac{\partial \psi}{\partial y}\frac{\partial N}{\partial x}-\frac{\partial \psi}{\partial x}\frac{\partial N}{\partial y}-\Big(1+\frac{K}{2}\Big)\frac{\partial^2 N}{\partial y^2}+K\Big(2N+\frac{\partial^2 \psi}{\partial y^2}\Big)=0, \tag{13}$$

$$\theta\frac{\partial T_1}{\partial t}+T_1\frac{\partial \theta}{\partial t}+\frac{\partial \psi}{\partial y}\Big(\theta\frac{\partial T_1}{\partial x}+T_1\frac{\partial \theta}{\partial x}\Big)-T_1\frac{\partial \psi}{\partial x}\frac{\partial \theta}{\partial y}-\frac{T_1}{Pr}\frac{\partial^2 \theta}{\partial y^2}+rT_1(\theta-1)=0, \tag{14}$$

where

$$M^*=\frac{\sigma L}{\rho \nu}, \quad r=\frac{4\Gamma L}{U_0 \rho c_p}.$$

The boundary conditions become

$$\begin{cases} t<0: \dfrac{\partial\psi}{\partial y}=0, \quad \dfrac{\partial\psi}{\partial x}=0, \quad N=0, \\ t>0: \dfrac{\partial\psi}{\partial y}=u_{\mathrm{w}}(x,t), \quad \dfrac{\partial\psi}{\partial x}=0, \quad N=-m_0\dfrac{\partial^2\psi}{\partial y^2}, \quad \theta=1 \quad \text{as} \quad y=0; \\ \qquad\quad \dfrac{\partial\psi}{\partial y}=0, \quad N=0, \quad \theta=0 \quad \text{as} \quad y\to\infty, \end{cases} \tag{15}$$

where $T_1=T_{\mathrm{w}}(x,t)-T_\infty$.

3 Group analysis and similarity equations

Our method of solutions depends on the application of a two-parameter group transformation to the partial differential equations (12)–(15). Under this transformation, the three independent variables will be reduced by two and the system of the partial differential equations (12)–(15) transforms into a system of ordinary differential equations in only one independent variable, i.e., which is the similarity variable.

The procedure is initiated with the group G, a class of transformations of the two-parameter "a_1, a_2" of the form

$$G: \begin{cases} \widetilde{S} \begin{cases} \tilde{x}=C^x x+K^x, \\ \tilde{y}=C^y y+K^y, \\ \tilde{t}=C^t t+K^t, \end{cases} \\ \tilde{\psi}=C^\psi\psi+K^\psi, \quad \tilde{\theta}=C^\theta\theta+K^\theta, \quad \widetilde{N}=C^N N+K^N, \\ \widetilde{T}_1=C^{T_1}T_1+K^{T_1}, \quad \widetilde{B}=C^B B+K^B, \quad \tilde{u}_{\mathrm{w}}=C^{u_{\mathrm{w}}}u_{\mathrm{w}}+K^{u_{\mathrm{w}}}. \end{cases} \tag{16}$$

The real valued functions C^S and K^S (S stands on x, y, t, ψ, θ, N, T_1, B, and u_{w}) are at least differentiable in their real arguments (a_1, a_2).

To transform the differential equations, the transformations of the derivatives are obtained from G via the chain-rule operations as follows:

$$\tilde{S}_{\tilde{i}}=\Big(\frac{C^S}{C^i}\Big)S_i, \quad \tilde{S}_{\tilde{i}\,\tilde{j}}=\Big(\frac{C^S}{C^iC^j}\Big)S_{ij}, \quad \tilde{S}_{\tilde{i}\,\tilde{j}\,\tilde{k}}=\frac{C^S}{C^iC^jC^k}S_{ijk}, \tag{17}$$

where $i=x,y,t$, $j=x,y,t$, $k=x,y,t$, and S stands for ψ, θ, T_1, N, and B.

Equations (12), (13), and (14) are said to be invariantly transformed under Eqs. (16) and (17) whenever

$$\begin{aligned} &\frac{\partial^2\tilde{\psi}}{\partial\tilde{y}\partial\tilde{t}}+\frac{\partial\tilde{\psi}}{\partial\tilde{y}}\frac{\partial^2\tilde{\psi}}{\partial\tilde{x}\partial\tilde{y}}-\frac{\partial\tilde{\psi}}{\partial\tilde{x}}\frac{\partial^2\tilde{\psi}}{\partial\tilde{y}^2}-(1+K)\frac{\partial^3\tilde{\psi}}{\partial\tilde{y}^3}-\widetilde{T}_1\tilde{\theta}-K\frac{\partial\widetilde{N}}{\partial\tilde{y}}+M^*\widetilde{B}^2(\tilde{x})\frac{\partial\tilde{\psi}}{\partial\tilde{y}} \\ &=H_1(a_1,a_2)\Big(\frac{\partial^2\psi}{\partial y\partial t}+\frac{\partial\psi}{\partial y}\frac{\partial^2\psi}{\partial x\partial y}-\frac{\partial\psi}{\partial x}\frac{\partial^2\psi}{\partial y^2}-(1+K)\frac{\partial^3\psi}{\partial y^3} \\ &\quad -T_1\theta-K\frac{\partial N}{\partial y}+M^*B^2(x)\frac{\partial\psi}{\partial y}\Big), \end{aligned} \tag{18}$$

$$\frac{\partial \widetilde{N}}{\partial \tilde{t}} + \frac{\partial \tilde{\psi}}{\partial \tilde{y}}\frac{\partial \widetilde{N}}{\partial \tilde{x}} - \frac{\partial \tilde{\psi}}{\partial \tilde{x}}\frac{\partial \widetilde{N}}{\partial \tilde{y}} - \Big(1+\frac{K}{2}\Big)\frac{\partial^2 \widetilde{N}}{\partial \tilde{y}^2} + K\Big(2\widetilde{N} + \frac{\partial^2 \tilde{\psi}}{\partial \tilde{y}^2}\Big)$$
$$= H_2(a_1,a_2)\Big(\frac{\partial N}{\partial t} + \frac{\partial \psi}{\partial y}\frac{\partial N}{\partial x} - \frac{\partial \psi}{\partial x}\frac{\partial N}{\partial y} - \Big(1+\frac{K}{2}\Big)\frac{\partial^2 N}{\partial y^2} + K\Big(2N + \frac{\partial^2 \psi}{\partial y^2}\Big)\Big), \tag{19}$$

$$\tilde{\theta}\frac{\partial \widetilde{T}_1}{\partial \tilde{t}} + \widetilde{T}_1\frac{\partial \tilde{\theta}}{\partial \tilde{t}} + \frac{\partial \tilde{\psi}}{\partial \tilde{y}}\Big(\tilde{\theta}\frac{\partial \widetilde{T}_1}{\partial \tilde{x}} + \widetilde{T}_1\frac{\partial \tilde{\theta}}{\partial \tilde{x}}\Big) - \widetilde{T}_1\frac{\partial \tilde{\psi}}{\partial \tilde{x}}\frac{\partial \tilde{\theta}}{\partial \tilde{y}}$$
$$- \frac{\widetilde{T}_1}{Pr}\frac{\partial^2 \tilde{\theta}}{\partial \tilde{y}^2} + r\widetilde{T}_1(\tilde{\theta}-1)$$
$$= H_3(a_1,a_2)\Big(\theta\frac{\partial T_1}{\partial t} + T_1\frac{\partial \theta}{\partial t} + \frac{\partial \psi}{\partial y}\Big(\theta\frac{\partial T_1}{\partial x} + T_1\frac{\partial \theta}{\partial x}\Big) - T_1\frac{\partial \psi}{\partial x}\frac{\partial \theta}{\partial y}$$
$$- \frac{T_1}{Pr}\frac{\partial^2 \theta}{\partial y^2} + rT_1(\theta-1)\Big), \tag{20}$$

where $H_1(a_1,a_2)$, $H_2(a_1,a_2)$, and $H_3(a_1,a_2)$ may be constants. Substituting Eqs. (16) and (17) into Eqs. (12), (13), and (14), we obtain

$$\frac{\partial^2 \tilde{\psi}}{\partial \tilde{y}\partial \tilde{t}} + \frac{\partial \tilde{\psi}}{\partial \tilde{y}}\frac{\partial^2 \tilde{\psi}}{\partial \tilde{x}\partial \tilde{y}} - \frac{\partial \tilde{\psi}}{\partial \tilde{x}}\frac{\partial^2 \tilde{\psi}}{\partial \tilde{y}^2} - (1+K)\frac{\partial^3 \tilde{\psi}}{\partial \tilde{y}^3}$$
$$- \widetilde{T}_1\tilde{\theta} - K\frac{\partial \widetilde{N}}{\partial \tilde{y}} + M^*\widetilde{B}^2(\tilde{x})\frac{\partial \tilde{\psi}}{\partial \tilde{y}} - R_1(a_1,a_2)$$
$$= H_1(a_1,a_2)\Big(\frac{\partial^2 \psi}{\partial y\partial t} + \frac{\partial \psi}{\partial y}\frac{\partial^2 \psi}{\partial x\partial y} - \frac{\partial \psi}{\partial x}\frac{\partial^2 \psi}{\partial y^2} - (1+K)\frac{\partial^3 \psi}{\partial y^3}$$
$$- T_1\theta - K\frac{\partial N}{\partial y} + M^*B^2(x)\frac{\partial \psi}{\partial y}\Big), \tag{21}$$

$$\frac{\partial \widetilde{N}}{\partial \tilde{t}} + \frac{\partial \tilde{\psi}}{\partial \tilde{y}}\frac{\partial \widetilde{N}}{\partial \tilde{x}} - \frac{\partial \tilde{\psi}}{\partial \tilde{x}}\frac{\partial \widetilde{N}}{\partial \tilde{y}} - \Big(1+\frac{K}{2}\Big)\frac{\partial^2 \widetilde{N}}{\partial \tilde{y}^2} + K\Big(2\widetilde{N} + \frac{\partial^2 \tilde{\psi}}{\partial \tilde{y}^2}\Big) - R_2(a_1,a_2)$$
$$= H_2(a_1,a_2)\Big(\frac{\partial N}{\partial t} + \frac{\partial \psi}{\partial y}\frac{\partial N}{\partial x} - \frac{\partial \psi}{\partial x}\frac{\partial N}{\partial y} - \Big(1+\frac{K}{2}\Big)\frac{\partial^2 N}{\partial y^2} + K\Big(2N + \frac{\partial^2 \psi}{\partial y^2}\Big)\Big), \tag{22}$$

$$\tilde{\theta}\frac{\partial \widetilde{T}_1}{\partial \tilde{t}} + \widetilde{T}_1\frac{\partial \tilde{\theta}}{\partial \tilde{t}} + \frac{\partial \tilde{\psi}}{\partial \tilde{y}}\Big(\tilde{\theta}\frac{\partial \widetilde{T}_1}{\partial \tilde{x}} + \widetilde{T}_1\frac{\partial \tilde{\theta}}{\partial \tilde{x}}\Big) - \widetilde{T}_1\frac{\partial \tilde{\psi}}{\partial \tilde{x}}\frac{\partial \tilde{\theta}}{\partial \tilde{y}}$$
$$- \frac{\widetilde{T}_1}{Pr}\frac{\partial^2 \tilde{\theta}}{\partial \tilde{y}^2} + r\widetilde{T}_1(\tilde{\theta}-1) - R_3(a_1,a_2)$$
$$= H_3(a_1,a_2)\Big(\theta\frac{\partial T_1}{\partial t} + T_1\frac{\partial \theta}{\partial t} + \frac{\partial \psi}{\partial y}\Big(\theta\frac{\partial T_1}{\partial x} + T_1\frac{\partial \theta}{\partial x}\Big)$$
$$- T_1\frac{\partial \psi}{\partial x}\frac{\partial \theta}{\partial y} - \frac{T_1}{Pr}\frac{\partial^2 \theta}{\partial y^2} + rT_1(\theta-1)\Big), \tag{23}$$

where

$$R_1(a_1,a_2) = \frac{K^B C^{\psi}}{C^y} - K^{T_1}C^{\theta}\theta - K^{\theta}C^{T_1}T_1 + K^{\theta}K^{T_1}, \tag{24}$$

$$R_2(a_1,a_2)=K^N, \tag{25}$$

$$R_3(a_1,a_2)=\frac{K^\theta C^{T_1}}{C^t}+\frac{K^\theta C^{T_1}C^\psi}{C^xC^y}+K^{T_1}C^\theta\theta+K^\theta C^{T_1}T_1-K^\theta K^{T_1}-K^{T_1}$$
$$+\frac{K^{T_1}C^\theta}{C^t}+\frac{K^{T_1}C^\theta C^\psi}{C^xC^y}+\frac{K^{T_1}C^\theta}{C^{y^2}}. \tag{26}$$

The invariance of Eqs. (21), (22), and (23) implies that $R_1(a_1,a_2)\equiv 0$, $R_2(a_1,a_2)\equiv 0$, $R_3(a_1,a_2)\equiv 0$, and

$$H_1(a_1,a_2)=\frac{C^\psi}{C^yC^t}=\frac{C^\psi}{(C^y)^2C^x}=\frac{C^\psi}{(C^y)^3}=\frac{C^N}{C^y}=\frac{C^BC^\psi}{C^y}, \tag{27}$$

$$H_2(a_1,a_2)=\frac{C^N}{C^t}=\frac{C^\psi C^N}{C^yC^x}=\frac{C^N}{(C^y)^2}=\frac{C^\psi}{(C^y)^2}=C^N, \tag{28}$$

$$H_3(a_1,a_2)=\frac{C^\theta C^{T_1}}{C^t}=\frac{C^\psi C^{T_1}C^\theta}{C^yC^x}=\frac{C^{T_1}C^\theta}{(C^y)^2}=C^\theta C^{T_1}=C^{T_1}. \tag{29}$$

The vanishing of R_1, R_2, and R_3 implies that

$$K^{T_1}=K^\theta=K^B=K^N=0. \tag{30}$$

The invariance of the boundary conditions (15) under the transformation (16) gives

$$K^y=K^{u_{\rm w}}=0,\quad C^\theta=1,\quad C^{u_{\rm w}}=\frac{C^\psi}{C^y},\quad C^N=\frac{C^\psi}{(C^y)^2}. \tag{31}$$

From Eqs. (27), (28), and (29) and invoking Eqs. (30) and (31), we get

$$C^y=C^t=C^B=1,\quad C^\psi=C^N=C^x=C^{T_1}=C^{u_{\rm w}}. \tag{32}$$

By substituting Eqs. (30)–(32) into Eq. (16), we get the group G. Then, transforming Eqs. (12)–(15) invariantly yields

$$G:\begin{cases}\widetilde{S}\begin{cases}\tilde{x}=C^xx+K^x,\\ \tilde{y}=y,\\ \tilde{t}=t+K^t,\end{cases}\\ \tilde{\psi}=C^x\psi+K^\psi,\quad \tilde{\theta}=\theta,\quad \widetilde{N}=C^xN,\\ \widetilde{T}_1=C^xT_1,\quad \widetilde{B}=B,\quad \tilde{u}_{\rm w}=C^xu_{\rm w}.\end{cases} \tag{33}$$

This group possesses complete sets of absolute invariants $\eta(x,y,t)$ and

$$g_i(x,y,t,\psi,\theta,T_1,N,B,u_{\rm w}),$$

where $i=1,2,\cdots,6$ are the six absolute invariants corresponding to ψ, θ, N, T_1, B, and $u_{\rm w}$.

3.1 Complete set of absolute invariants

The complete set of absolute invariants consists of the absolute invariants of the independent variables x, y, and t and the absolute invariants of the dependent variables ψ, θ, N, T_1, B, and $u_{\rm w}$.

If $\eta(x, y, t)$ is the absolute invariant of independent variables, then

$$g_i(x, y, t, \psi, \theta, T_1, N, B, u_{\rm w}) = F_i(\eta(x, y, t)) \ (i = 1, 2, \cdots, 6)$$

are the dependant absolute invariants.

The dependent and independent similarity variables are obtained by applying the Morgan theorem[16], which states that a function $g_i(x, y, t, \psi, \theta, T_1, N, B, u_{\rm w})$ is an absolute invariant of a two-parameter group if and only if it satisfies the following two first-order linear differential equations:

$$\begin{cases} \displaystyle\sum_{i=1}^{9}(\alpha_i\xi_i + \alpha_{i+1})\frac{\partial g_i}{\partial \xi_i} = 0, \\ \displaystyle\sum_{i=1}^{9}(\beta_i\xi_i + \beta_{i+1})\frac{\partial g_i}{\partial \xi_i} = 0, \end{cases} \tag{34}$$

where ξ_i stand for $x, y, t, \psi, \theta, T_1, N, B$, and $u_{\rm w}$, respectively, and α_i and β_i are defined by the relations

$$\begin{cases} \alpha_1 = \Big(\dfrac{\partial C^x}{\partial a_1}\Big)_{(a_1^0, a_2^0)}, \quad \alpha_2 = \Big(\dfrac{\partial K^x}{\partial a_1}\Big)_{(a_1^0, a_2^0)}, \quad \alpha_3 = \Big(\dfrac{\partial C^y}{\partial a_1}\Big)_{(a_1^0, a_2^0)}, \quad \cdots, \\ \beta_1 = \Big(\dfrac{\partial C^x}{\partial a_2}\Big)_{(a_1^0, a_2^0)}, \quad \beta_2 = \Big(\dfrac{\partial K^x}{\partial a_2}\Big)_{(a_1^0, a_2^0)}, \quad \beta_3 = \Big(\dfrac{\partial C^y}{\partial a_2}\Big)_{(a_1^0, a_2^0)}, \quad \cdots, \end{cases} \tag{35}$$

where (a_1^0, a_2^0) denotes the value of "a_1, a_2", which yields the identity element of the group.

3.1.1 Invariant transformation of independent variables

We first deduce the similarity variable $\eta(x, y, t)$ as follows:

$$\begin{cases} (\alpha_1 x + \alpha_2)\dfrac{\partial \eta}{\partial x} + (\alpha_3 y)\dfrac{\partial \eta}{\partial y} + (\alpha_5 t + \alpha_6)\dfrac{\partial \eta}{\partial t} = 0, \\ (\beta_1 x + \beta_2)\dfrac{\partial \eta}{\partial x} + (\beta_3 y)\dfrac{\partial \eta}{\partial y} + (\beta_5 t + \beta_6)\dfrac{\partial \eta}{\partial t} = 0. \end{cases} \tag{36}$$

Since $K^y = 0$, according to the definition of α_i and β_i,

$$\alpha_4 = \beta_4 = 0. \tag{37}$$

Eliminating $y\frac{\partial \eta}{\partial y}$ and $\frac{\partial \eta}{\partial x}$ from Eq. (36) yields

$$\begin{cases} (\lambda_{13}x + \lambda_{23})\dfrac{\partial \eta}{\partial x} + (\lambda_{53}t + \lambda_{63})\dfrac{\partial \eta}{\partial t} = 0, \\ (\lambda_{31}x + \lambda_{32})y\dfrac{\partial \eta}{\partial y} + (\lambda_{51}xt + \lambda_{61}x + \lambda_{52}t + \lambda_{62})\dfrac{\partial \eta}{\partial t} = 0, \end{cases} \tag{38}$$

where

$$\lambda_{ij} = \alpha_i\beta_j - \alpha_j\beta_i, \quad i, j = 1, 2, \cdots, 6. \tag{39}$$

According to the basic theorem of the group theory, Eq. (38) has one and only one solution if the coefficient matrix has the rank two. The matrix has the rank two whenever at least one of its two by two submatrices has a nonvanishing determinant. This condition is met whenever at least one of the following is satisfied:

$$\lambda_{13}x + \lambda_{22} \neq 0, \quad \lambda_{35}t + \lambda_{36} \neq 0, \quad \text{or} \quad \lambda_{15}xt + \lambda_{16}x + \lambda_{25}t + \lambda_{26} \neq 0. \tag{40}$$

According to the definition of the class G of the two-parameter group (33) and the definitions of α_i and β_i, we have

$$\lambda_{31} = \lambda_{32} = \lambda_{35} = \lambda_{36} = \lambda_{15} = \lambda_{25} = 0. \tag{41}$$

Then, according to the condition (40), the first equation of Eq. (38) is satisfied, but the second equation is reduced to

$$\frac{\partial \eta}{\partial t} = 0. \tag{42}$$

Then, from Eq. (38), we can deduce that

$$(\lambda_{16} x + \lambda_{26}) \frac{\partial \eta}{\partial x} = 0. \tag{43}$$

From Eqs. (42) and (43), the similarity variable η has the form

$$\eta = f(y). \tag{44}$$

Without loss of generality, the independent absolute invariant $\eta(y)$ in Eq. (44) may be assumed in the form

$$\eta = Ay. \tag{45}$$

3.1.2 Absolute invariants of dependent variables

Similarly, we can find absolute invariants of the dependent variables. We mention that θ and B are themselves absolute invariants. Thus, $\theta(x, y, t) = \theta(\eta)$ and $B(x) = B(\eta)$. Since η does not depend on x, it is convenient for $B(x)$ to be a constant, i.e., $B(x) = B_0$. Equation (34) may be solved to get the other four absolute invariants. Frequently, the following forms corresponding to ψ, T_1, N, B, and $u_{\rm w}$ may be assumed:

$$\begin{cases} \psi(x, y, t) = \Gamma_1(x, t) f(\eta), \quad T_1(x, t) = \Gamma_2(x, t) E(\eta), \\ N(x, y, t) = \Gamma_3(x, t) I(\eta), \quad u_{\rm w}(x, t) = \Gamma_4(x, t) G(\eta) \end{cases} \tag{46}$$

since $u_{\rm w}(x, t)$ and $T_1(x, t)$ are independent of y whereas η depends on y. It follows that $E(\eta)$ and $G(\eta)$ must be equal to constants, which are denoted by T_0 and $U_{\rm r}$, respectively. Thus, Eq. (46) becomes

$$\begin{cases} \psi(x, y, t) = \Gamma_1(x, t) f(\eta), \quad \theta(x, y, t) = \theta(\eta), \\ T_1(x, t) = T_0 \Gamma_2(x, t), \quad N(x, y, t) = \Gamma_3(x, t) I(\eta), \\ u_{\rm w}(x, t) = U_{\rm r} \Gamma_4(x, t), \quad B(x) = B_0. \end{cases} \tag{47}$$

The reduction of Eqs. (12)–(15) to ordinary differential equations depends on the forms of Γ_1, Γ_2, Γ_3, and Γ_4.

3.2 Reduction to ordinary differential equations

Substituting Eq. (47) into Eqs. (12)–(15), we have

$$(1 + K) f''' + c_1 (f f'' + f'^2) - c_2 f' + c_3 \theta + K c_4 I' - M f' = 0, \tag{48}$$

$$\Big(1 + \frac{K}{2}\Big) f''' + c_1 I' f - c_5 f' I - c_6 I - K \Big(2I + \frac{f''}{c_4}\Big) = 0, \tag{49}$$

$$\frac{1}{Pr} \theta'' + c_1 \theta' f - c_7 f' \theta - c_8 \theta - r(\theta - 1) = 0 \tag{50}$$

with the boundary conditions

$$\begin{cases} \eta = 0: \ f' = c_9, \quad f = 0, \quad I = -\dfrac{m_0}{c_4} f'', \quad \theta = 1, \\ \eta \to \infty: \ f' \to 0, \quad I \to 0, \quad \theta \to 0, \end{cases} \tag{51}$$

where

$$\begin{cases} c_1 = \dfrac{\partial \Gamma_1}{\partial x}, \quad c_2 = \dfrac{1}{\Gamma_1}\dfrac{\partial \Gamma_1}{\partial t}, \quad c_3 = \dfrac{T_0 \Gamma_2}{\Gamma_1}, \quad c_4 = \dfrac{\Gamma_3}{\Gamma_1}, \quad c_5 = \dfrac{\Gamma_1}{\Gamma_3}\dfrac{\partial \Gamma_3}{\partial x}, \\ c_6 = \dfrac{1}{\Gamma_3}\dfrac{\partial \Gamma_3}{\partial t}, \quad c_7 = \dfrac{\Gamma_1}{\Gamma_2}\dfrac{\partial \Gamma_2}{\partial x}, \quad c_8 = \dfrac{1}{\Gamma_2}\dfrac{\partial \Gamma_2}{\partial t}, \quad c_9 = \dfrac{U_{\rm r}\Gamma_4}{\Gamma_1}. \end{cases} \tag{52}$$

It is necessary that the coefficients c_i $(i = 1, 2, \cdots, 9)$ are constants or functions of η only. Several trials on possible values of c_i only lead to two distinct cases:

(i) Γ_1 depends only on x $(\Gamma_1 = \Gamma_1(x))$.

(ii) Γ_1 depends only on t $(\Gamma_1 = \Gamma_1(t))$.

3.2.1 Reduction to ordinary differential equations when $\Gamma_1 = \Gamma_1(x)$

For this case and from Eq. (52), we get

$$\begin{cases} c_2 = c_7 = c_8 = 0, \quad c_1 = c_5 = c_7, \quad \Gamma_1 = c_1 x + k_1, \\ \Gamma_2 = \dfrac{c_3}{T_0}(c_1 x + k_1), \quad \Gamma_3 = c_4(c_1 x + k_1), \quad \Gamma_4 = \dfrac{c_9}{U_{\rm r}}(c_1 x + k_1), \end{cases} \tag{53}$$

where k_1 is an integration constant. Then, Eqs. (48)–(50) have the forms as follows:

$$(1+K)f''' + c_1(ff'' + f'^2) + c_3\theta + Kc_4 I' - Mf' = 0, \tag{54}$$

$$\Big(1+\frac{K}{2}\Big)I'' + c_1(I'f - f'I) - K\Big(2I + \frac{f''}{c_4}\Big) = 0, \tag{55}$$

$$\frac{1}{Pr}\theta'' + c_1(\theta' f - f'\theta) - r(\theta - 1) = 0 \tag{56}$$

subjected to the boundary conditions (51), and the forms of η, ψ, θ, $T_{\rm w}$, N, B, and $u_{\rm w}$ are

$$\begin{cases} \eta = y, \quad \psi(x, y, t) = (c_1 x + k_1) f(\eta), \\ T_{\rm w}(x, t) = T_\infty + c_3(c_1 x + k_1), \quad N(x, y, t) = c_4(c_1 x + k_1) I(\eta), \\ u_{\rm w}(x, t) = c_9(c_1 x + k_1), \quad \theta(x, y, t) = \theta(\eta), \quad B(x) = B_0. \end{cases} \tag{57}$$

3.2.2 Reduction to ordinary differential equations when $\Gamma_1 = \Gamma_1(t)$

For this case and from Eq. (52), we get

$$\begin{cases} c_1 = c_5 = c_7 = 0, \quad c_2 = c_6 = c_8, \quad \Gamma_1 = k_2 {\rm e}^{c_2 t} f(\eta), \\ \Gamma_2 = \dfrac{c_3}{T_0} k_2 {\rm e}^{c_2 t}, \quad \Gamma_3 = c_4 k_2 {\rm e}^{c_2 t}, \quad \Gamma_4 = \dfrac{c_9}{U_{\rm r}} k_2 {\rm e}^{c_2 t}, \end{cases} \tag{58}$$

where k_2 is an integration constant. Then, Eqs. (48)–(50) have the forms as follows:

$$(1+K)f''' - c_2 f' + c_3\theta + Kc_4 I' - Mf' = 0, \tag{59}$$

$$\Big(1+\frac{K}{2}\Big)I'' - c_2 I - K\Big(2I + \frac{f''}{c_4}\Big) = 0, \tag{60}$$

$$\frac{1}{Pr}\theta'' - c_2\theta - r(\theta - 1) = 0 \tag{61}$$

subjected to the boundary conditions (51), and the forms of η, ψ, θ, $T_{\rm w}$, N, B, and $u_{\rm w}$ are

$$\begin{cases} \eta = y, \quad \psi(x,y,t) = k_2 \mathrm{e}^{c_2 t} f(\eta), \\ T_{\rm w}(x,t) = T_\infty + c_3 k_2 \mathrm{e}^{c_2 t}, \\ N(x,y,t) = c_4 k_2 \mathrm{e}^{c_2 t} I(\eta), \\ \theta(x,y,t) = \theta(\eta), \quad u_{\rm w}(x,t) = c_9 k_2 \mathrm{e}^{c_2 t}, \quad B(x) = B_0. \end{cases} \tag{62}$$

The domain of the governing boundary layer equations is the unbounded region $[0,\infty)$. However, for all practical reasons, the governing boundary layer equations (59)–(61) have the domain $0 \leqslant \eta \leqslant \eta_\infty$, where η_∞ is one end of the user specified computational domain. The set of nonlinear ordinary differential equations (59) and (61) with the boundary conditions (51) has analytical solutions for $K = 0$ and $c_9 = 1$, these solutions are shown in Appendix A.

In technological applications, the skin-friction coefficient, the couple stress coefficient at the wall, and the Nusselt number are important quantities that are of practical interest. These quantities are, respectively, given by

$$\frac{1}{2} C_{\rm f} Re^{\frac{1}{2}} u_{\rm w} = -(1 + (1 + m_0)K) f''(0), \tag{63}$$

$$C_{\rm w} Re\, u_{\rm w} = \Big(1 + \frac{K}{2}\Big) I'(0), \tag{64}$$

$$Nu Re^{-\frac{1}{2}} = -\theta'(0). \tag{65}$$

4 Numerical solutions

The nonlinear ordinary differential equations (59)–(61) with the boundary conditions (51) described the unsteady case are solved numerically by the Chebyshev spectral method[17–18]. Now, we display the major concepts for solving ordinary differential equations by the Chebyshev function and the following algebraic mapping:

$$\zeta = \frac{2\eta}{\eta_\infty} - 1, \tag{66}$$

and map the bounded region $0 \leqslant \eta \leqslant \eta_\infty$ to the the finite domain $[-1,1]$. Then, Eqs. (59)–(61) have the forms

$$(1+K)\Big(\frac{2}{\eta_\infty}\Big)^3 f'''(\zeta) - \frac{2}{\eta_\infty} c_2 f'(\zeta) + c_3 \theta(\zeta) + \frac{2}{\eta_\infty} K c_4 I'(\zeta) - \frac{2}{\eta_\infty} M f'(\zeta) = 0, \tag{67}$$

$$\Big(1 + \frac{K}{2}\Big)\Big(\frac{2}{\eta_\infty}\Big)^2 I''(\zeta) - c_2 I(\zeta) - K\Big(2I(\zeta) + \Big(\frac{2}{\eta_\infty}\Big)^2 \frac{f''(\zeta)}{c_4}\Big) = 0, \tag{68}$$

$$\frac{1}{Pr}\Big(\frac{2}{\eta_\infty}\Big)^2 \theta''(\zeta) - c_2 \theta(\zeta) - r(\theta(\zeta) - 1) = 0 \tag{69}$$

with the transformed boundary conditions as follows:

$$\begin{cases} \zeta = -1: \ f' = \dfrac{\eta_\infty}{2} c_9, \quad f = 0, \quad I = -\dfrac{m_0}{c_4}\Big(\dfrac{2}{\eta_\infty}\Big)^2 f'', \quad \theta = 1, \\ \zeta = 1: \ f' = 0, \quad I = 0, \quad \theta = 0. \end{cases} \tag{70}$$

By applying the Chebyshev method on Eqs. (67)–(69) with the boundary condition (70), we get a nonlinear algebraic system of equations as follows:

$$(1+K)\Big(\frac{2}{\eta_\infty}\Big)^3\phi_i - \frac{2c_2}{\eta_\infty}\Big(\sum_{j=0}^{n}L_{ij}^1\phi_j + d_i^1\Big) + c_3\Big(\sum_{j=0}^{n}L_{ij}^2\chi_j + q_i^2\Big)$$
$$+\frac{2Kc_4}{\eta_\infty}\Big(\sum_{j=0}^{n}L_{ij}^1\psi_j + \sum_{j=0}^{n}N_{ij}^1\phi_j + r_i^1\Big) - \frac{2M}{\eta_\infty}\Big(\sum_{j=0}^{n}L_{ij}^2\phi_j + d_i^2\Big) = 0, \tag{71}$$

$$\Big(1+\frac{K}{2}\Big)\Big(\frac{2}{\eta_\infty}\Big)^2\psi_i - c_2\Big(\sum_{j=0}^{n}L_{ij}^2\psi_j + \sum_{j=0}^{n}N_{ij}^2\phi_j + r_i^2\Big)$$
$$-K\Big(2\Big(\sum_{j=0}^{n}L_{ij}^2\psi_j + \sum_{j=0}^{n}N_{ij}^2\phi_j + r_i^2\Big) + \frac{2}{\eta_\infty c_4}\Big(\sum_{j=0}^{n}L_{ij}^1\phi_j + d_i^1\Big)\Big) = 0, \tag{72}$$

$$\frac{1}{Pr}\Big(\frac{2}{\eta_\infty}\Big)^2\chi_i - c_2\Big(\sum_{j=0}^{n}L_{ij}^2\chi_j + q_i^2\Big) - r\Big(\sum_{j=0}^{n}L_{ij}^2\chi_j + q_i^2 - 1\Big) = 0, \tag{73}$$

where

$$\begin{cases} L_{ij}^1 = b_{ij} - \dfrac{1}{2}b_{nj}^2, \quad d_i^1 = -\dfrac{c_9\eta_\infty}{4}, \\ L_{ij}^2 = b_{ij}^2 - \dfrac{\zeta_i+1}{2}b_{nj}^2, \quad d_i^2 = -\dfrac{1}{4}c_9(\zeta_i+1)\eta_\infty + \dfrac{1}{2}c_9\eta_\infty, \\ L_{ij}^3 = b_{ij}^3 - \dfrac{(\zeta_i+1)^2}{4}b_{nj}^2, \quad d_i^3 = -\dfrac{1}{8}c_9(\zeta_i+1)^2\eta_\infty + \dfrac{1}{2}c_9\eta_\infty(\zeta_i+1), \\ N_{ij}^1 = -\dfrac{m_0}{2}\Big(\dfrac{2}{\eta_\infty}\Big)^2 b_{nj}^2, \quad r_i^1 = -\dfrac{c_9 m_0}{2\eta_\infty}, \\ N_{ij}^2 = \dfrac{m_0}{2}\Big(\dfrac{2}{\eta_\infty}\Big)^2 b_{nj}^2 - \dfrac{m_0(\zeta_i+1)}{4}\Big(\dfrac{2}{\eta_\infty}\Big)^2 b_{nj}^2, \\ r_i^2 = -\dfrac{m_0(\zeta_i+1)}{2\eta_\infty} + \dfrac{m_0 c_9}{\eta_\infty}, \\ q_i^1 = -\dfrac{1}{2}, \quad q_i^2 = 1 - \dfrac{\zeta_i+1}{2}. \end{cases} \tag{74}$$

Here, b_{ij}, $b_{ij}^{(2)}$, and $b_{ij}^{(3)}$ are elements in the $(n+1)$ square matrices defined in Ref. [17]. This system of nonlinear equations is solved by Newton's iteration for the unknown ϕ_i, ψ_i, and χ_i $(i = 0, \cdots, n)$.

5 Discussion

To assess the accuracy of the numerical method, we compare our results for Eqs. (59) and (61) subjected to the boundary condition (51) with the analytical results which are presented in Appendix A with $c_2 = 1$, $\eta_\infty = 10$, $K = 0$, and $c_9 = 1$. As shown in Table 1, the comparison shows good agreement. The resulting equations (59)–(61) with the boundary conditions (51) are solved numerically by a Chebyshev spectral method discussed in the previous section with $c_2 = c_4 = c_9 = 1$ and the assumption that $c_3 = \lambda$ is the mixed convection parameter.

Table 1 Analytical and numerical results of $-f''(0)$ and $-\theta'(0)$ with $c_2 = 1$, $K = 0$, $c_9 = 1$, and $\eta_\infty = 10$

Pr	M	c_3	r	$-f''(0)$		$-\theta'(0)$	
				Analytical	Numerical	Analytical	Numerical
0.72	0.5	0.10	0.02	1.176 05	1.176 05	0.840 174	0.840 174
1.00	0.5	0.30	0.01	1.089 11	1.089 11	0.995 038	0.995 038
0.72	0.5	0.01	0.01	1.219 90	1.219 90	0.844 320	0.844 320
3.00	1.0	0.20	0.02	1.405 50	1.405 50	1.714 990	1.714 990

Figures 2 and 3 illustrate the effects of the material parameter K on the velocity f' and the angular velocity I, respectively. It can be seen from Fig. 2 that the velocity increases as the material parameter K increases near the surface and decreases with the increase in K away from the surface. Also, one can observe that f' remains positive near the boundary whereas negative away from the boundary. Figure 3 displays that for $m_0 = 0.5$, the micro-rotation velocity I decreases with the increase in K near the plate, while increases with the increase in K away from the surface. Also, for $m_0 = 0.0$, the micro-rotation velocity I increases with the increase in K.

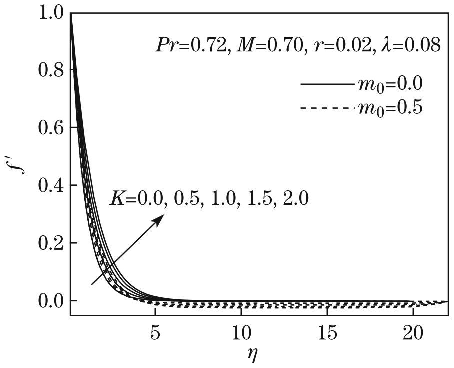

Fig. 2 Velocity profiles for various K

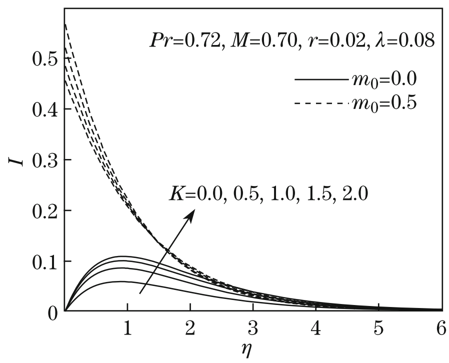

Fig. 3 Angular velocity profiles for various K

Figure 4 shows the effects of the radiation parameter r on the temperature profiles. It is observed that the temperature increases as the radiation parameter r increases. This result qualitatively agrees with the expectation since the effects of the radiation and the surface temperature are to increase the rate of the energy transport to the fluid and accordingly to increase the temperature of the fluid.

Figures 5–7 illustrate the variations of the velocity f' and the angular velocity profiles I with the magnetic parameter M. Figure 5 depicts the variations of f' with M. It is observed that f' decreases with the increase in M along the surface. This is because that the application of a transverse magnetic field to an electrically conducting fluid gives rise to a resistive-type force called the Lorentz force. This force has the tendency to slow down the motion of the fluid in the boundary layer. The profiles of the angular velocity I with various M for $m_0 = 0.0$ and $m_0 = 0.5$ are shown in Figs. 6 and 7, respectively. It is clear from Fig. 6 that for $m_0 = 0.0$, the angular velocity I decreases with an increase in M near the surface and increases with the increase in M away from the surface. Figure 7 depicts that for $m_0 = 0.5$, the angular velocity I increases with an increase in M near the surface and decreases with the increase in M away from the surface.

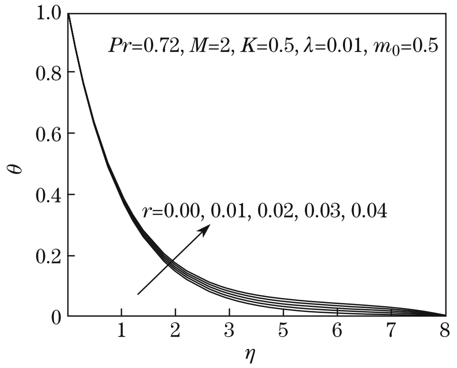

Fig. 4 Temperature profiles for various r

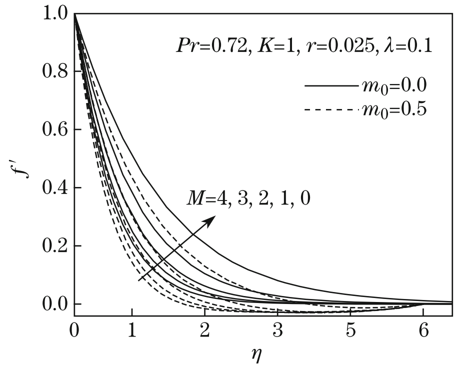

Fig. 5 Velocity profiles for various M

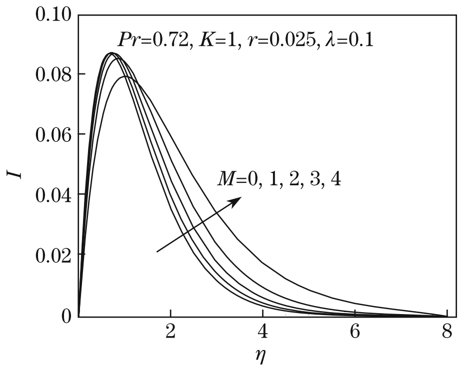

Fig. 6 Angular velocity profiles for various M with $m_0 = 0.0$

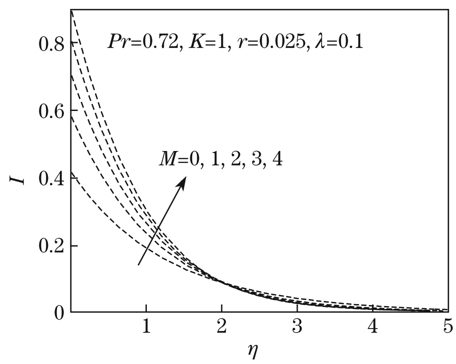

Fig. 7 Angular velocity profiles for various M with $m_0 = 0.5$

Figures 8 and 9 depict the effects of the Prandtl number Pr on f' and θ, respectively. It is seen that f' and θ decrease as Pr increases. This is in agreement with the fact that the thermal boundary layer thickness decreases with the increase in Pr.

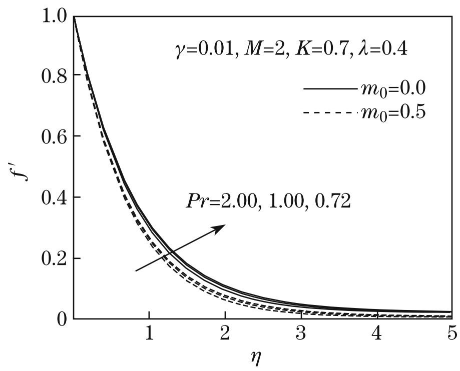

Fig. 8 Velocity profiles for various Pr

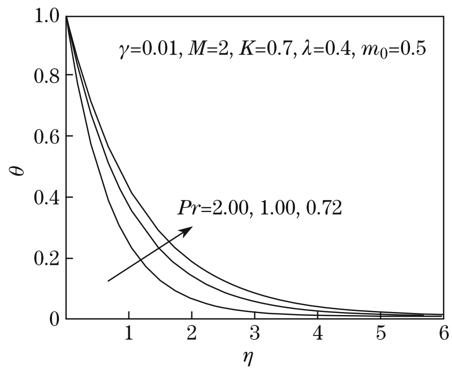

Fig. 9 Temperature profiles for various Pr

It is observed from Fig. 10 that the velocity increases for large values of λ while the boundary layer thickness is the same for all values of λ.

Figures 11 and 12 present the skin-friction coefficient and the wall couple stress coefficient for different values of K and M while the other parameters are fixed. It is noticed from Fig. 11 that the skin-friction coefficient increases with the increase in K at a fixed value of M and the skin-friction coefficient increases with the increase in M at a fixed value of K. Also, Fig. 12 shows that the wall couple stress coefficient decreases as K increases at a fixed value of M for $m_0 = 0.5$, and the reverse is true for $m_0 = 0.0$. While at a fixed value of K, the wall couple stress coefficient increases as M increases for $m_0 = 0.5$, and the reverse is true for $m_0 = 0.0$.

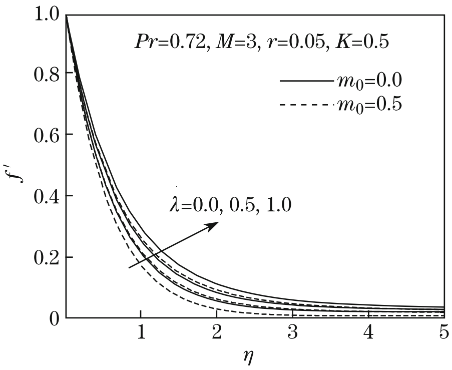

Fig. 10 Velocity profiles for various λ

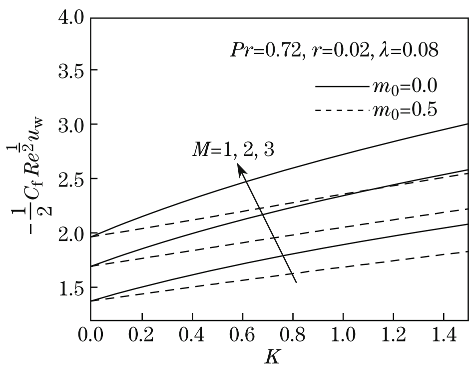

Fig. 11 Skin-friction coefficient as function of K for various M

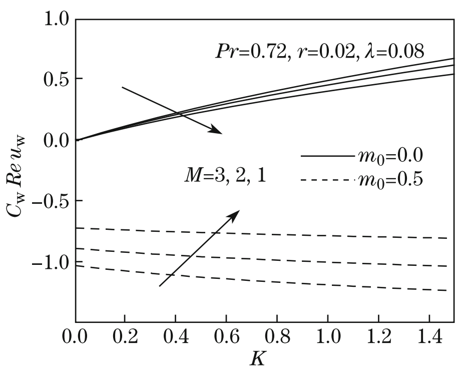

Fig. 12 Wall couple stress coefficient as function of K for various M

Figures 13 and 14 present the skin-friction coefficient and the Nusselt number for different values of r and Pr while all other parameters are fixed. It is noticed that as r increases, the skin-friction coefficient and the Nusselt number decrease considerably for a fixed value of Pr. Also, it is seen that as Pr increases, the skin-friction coefficient and the Nusselt number increase considerably for a fixed value of r.

Figures 15 and 16 present the skin-friction coefficient and the Nusselt number for different values of K and λ while all other parameters are fixed. It is found that the skin-friction coefficient decreases with the increase in λ at a fixed value of K. While the wall couple stress increases with the increase in λ at a fixed value of K for $m_0 = 0.5$, and the reverse is true for $m_0 = 0.0$.

6 Conclusions

In the present work, the most widely applicable method for transforming a system of partial differential equations into an invariant system of ordinary differential equations utilizes the

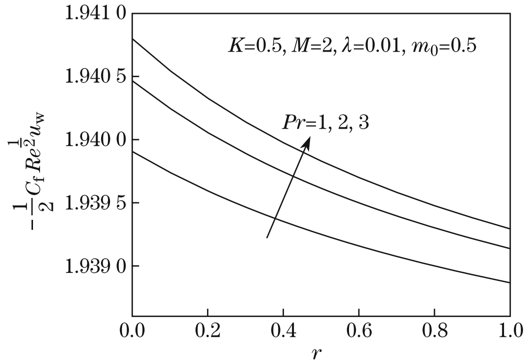

Fig. 13 Skin-friction coefficient as function of r for various Pr

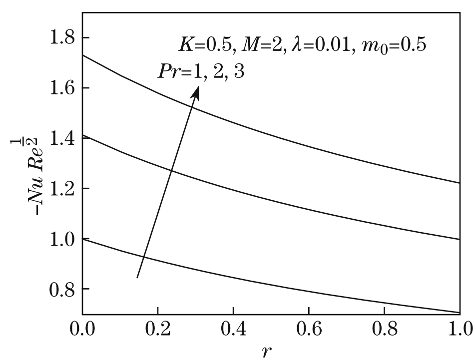

Fig. 14 Nusselt number as function of r for various Pr

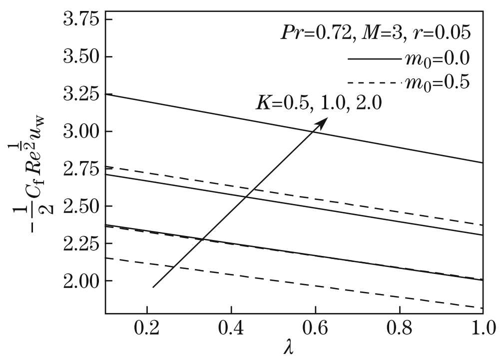

Fig. 15 Skin-friction coefficient as function of λ for various K

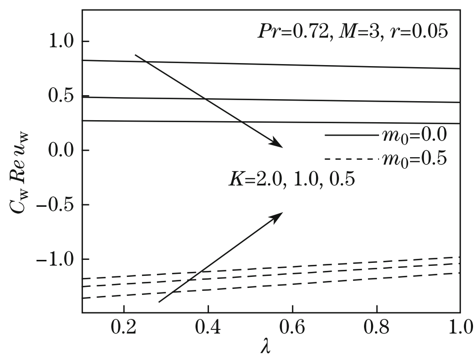

Fig. 16 Wall couple stress coefficient as function of λ for various K

underlying group structure to solve the problem of an unsteady MHD micropolar fluid. This fluid flows over a vertical nonisothermal stretching surface with the radiation effect. We obtain two systems of ordinary differential equations. One represents the steady case, and the other represents the unsteady case. The system represented the unsteady case is solved numerically by the Chebyshev spectral method. The velocity, the angular velocity, the temperature field, the local skin-friction coefficient, and the local Nusselt number are presented for various values of the parameters governing the problem by considering $m_0 = 0.0$ and $m = 0.5$.

We observed that the velocity f' increases with the increases in the material parameter K, the Prandtl number Pr, and the mixed convection parameter λ, while it decreases with the increase in M. The temperature θ increases with the increase in the radiation parameter r and decreases with the increase in the Prandtl number Pr. Moreover, the skin-friction coefficient increases with the increases in K, M, and Pr, while it decreases with the increases in λ and r.

Acknowledgments The authors thank the referees for their valuable comments which improve the paper and for their great interest in this work.

References

[1] Hayat, T., Abbas, Z., and Javed, T. Mixed convection flow of a micropolar fluid over a non-linearly stretching sheet. *Physics Letters A*, **372**, 637–647 (2008)

[2] Ishak, A. Thermal boundary layer flow over a stretching sheet in a micropolar fluid with radiation effect. *Meccanica*, **45**, 367–373 (2010)

[3] Mahmoud, M. A. A. and Waheed, S. E. MHD flow and heat transfer of a micropolar fluid over a nonlinear stretching surface with variable surface heat flux and heat generation. *Canadian Journal of Chemical Engineering*, **89**, 1408–1415 (2011)

[4] Eringen, A. Simple microfluids. *International Journal of Engineering Science*, **2**, 205–217 (1964)

[5] Eringen, A. Theory of micropolar fluids. *Journal of Mathematics and Mechanics*, **16**, 1–18 (1966)

[6] Eringen, A. Theory of thermomicropolar fluids. *Journal of Mathematical Analysis and Applications*, **9**, 480–496 (1972)

[7] Agarwal, R. S. and Dhanapal, C. Numerical solution of unsteady flow and heat transfer in a micropolar fluid past a porous flat plate. *Indian Journal of Pure and Applied Mathematics*, **20**, 513–520 (1989)

[8] Damesh, R. A., Al-Azab, T. A., Shannak, B. A., and Al-Husein, M. Unsteady natural convection heat transfer of micropolar fluid over a vertical surface with constant heat flux. *Turkish Journal of Engineering and Environmental Sciences*, **31**, 225–233 (2007)

[9] Nazar, R., Ishak, A., and Pop, I. Unsteady boundary layer flow over a stretching sheet in a micropolar fluid. *International Journal of Engineering and Natural Sciences*, **2**, 161–165 (2008)

[10] Nazar, R., Ishak, A., Darus, M., and Pop, I. Unsteady boundary layer flow and heat transfer over a stretching surface in a micropolar fluid. *Proceedings of the 13th WSEAS International Conference on Applied Mathematics (Math'08)*, World Scientific and Engineering Academy and Society (WSEAS) Stevens Point, Wisconsin, 273–278 (2008)

[11] Bachok, N., Ishak, A., and Nazar, R. Flow and heat transfer over an unsteady stretching sheet in a micropolar fluid. *Meccanica*, **46**, 935–942 (2011)

[12] Ibrahim, F. S. and Hamad, M. A. A. Group method analysis of mixed convection boundary-layer flow of a micropolar fluid near a stagnation point on a horizontal cylinder. *Acta Mechanica*, **181**, 65–81 (2006)

[13] Abd-Elaziz, M. M. and Ahmed, S. E. Group solution for unsteady boundary layer flow of a micropolar fluid near the rear stagnation point of a plane surface in a porous medium. *Latin American Applied Research*, **38**, 161–168 (2008)

[14] Hassanien, I. A. and Hamad, M. A. Group theoretic method for unsteady free convection flow of a micropolar fluid along a vertical plate in a thermally stratified medium. *Applied Mathematical Modelling*, **32**, 1099–1114 (2008)

[15] Chamkha, A. J., Mohamed, R. A., and Ahmed, S. E. Unsteady MHD natural convection from a heated vertical porous plate in a micropolar fluid with Joule heating, chemical reaction and radiation effects. *Meccanica*, **46**, 399–411 (2011)

[16] Moran, M. J. and Gaggioli, R. A. A new systematic formalism for similarity analysis. *Journal of Engineering Mathematics*, **3**, 151–162 (1969)

[17] El-Gendi, S. E. On Chebyshev solution of parabolic partial differential equations. *Journal of the Institute of Mathematics and Its Applications*, **16**, 283–289 (1975)

[18] Hassanien, I. A., El-Hawary, H. M., and Salama, A. A. Chebyshev solution of axisymmetric stagnation flow on a cylinder. *Energy Conversion and Management*, **37**, 67–76 (1996)

Appendix A

The analytical solution is as follows:

$$\lambda_1 = c_2 + M, \quad \lambda_2 = (c_2 + r)Pr, \quad \lambda_3 = rPr,$$

$$\begin{aligned} f(\eta) = {} & \frac{1}{4\lambda_1^{\frac{3}{2}}(\lambda_1-\lambda_2)\lambda_2^{\frac{3}{2}}}\Big(\mathrm{e}^{-2\eta(\sqrt{\lambda_1}+\sqrt{\lambda_2})}(-1+\coth(\eta_\infty\sqrt{\lambda_1}))(-1+\coth(\eta_\infty\sqrt{\lambda_2})) \\ & \cdot\Big(8\mathrm{e}^{(2\eta+\eta_\infty)(\sqrt{\lambda_1}+\sqrt{\lambda_2})}\sinh\frac{\eta\sqrt{\lambda_1}}{2}\sinh(\eta_\infty\sqrt{\lambda_2})\lambda_2^{\frac{3}{2}}\Big(\sinh\Big(\frac{1}{2}(\eta-2\eta_\infty)\sqrt{\lambda_1}\Big)\lambda_1(c_3-\lambda_1+\lambda_2) \\ & + c_3\Big(\sinh\frac{\eta\sqrt{\lambda_1}}{2} - \sinh\Big(\frac{1}{2}(\eta-2\eta_\infty)\sqrt{\lambda_1}\Big)\Big)\lambda_3\Big) \end{aligned}$$

$$+ c_3(-1+e^{2\eta_\infty\sqrt{\lambda_1}})\sqrt{\lambda_1}(-e^{2\eta(\sqrt{\lambda_1}+\sqrt{\lambda_2})}(-1+e^{2\eta_\infty\sqrt{\lambda_2}})\eta\lambda_2^{\frac{3}{2}}\lambda_3$$
$$+ 2e^{2\eta\sqrt{\lambda_1}+(2\eta+\eta_\infty)\sqrt{\lambda_2}}\lambda_1((-\cosh((\eta-\eta_\infty)\sqrt{\lambda_2})+\cosh(\eta_\infty\sqrt{\lambda_2}))\lambda_2$$
$$+ (1-\cosh(\eta\sqrt{\lambda_2})+\cosh((\eta-\eta_\infty)\sqrt{\lambda_2})$$
$$- \cosh(\eta_\infty\sqrt{\lambda_2})+\eta\sinh(\eta_\infty\sqrt{\lambda_2})\sqrt{\lambda_2})\lambda_3))\Big)\Big),$$

$$f'(\eta) = -\frac{1}{4\lambda_1(\lambda_1-\lambda_2)\lambda_2}(e^{-2\eta(\sqrt{\lambda_1}+\sqrt{\lambda_2})}(-1+\coth(\eta_\infty\sqrt{\lambda_1}))(-1+\coth(\eta_\infty\sqrt{\lambda_2}))$$
$$\cdot (c_3e^{\eta(\sqrt{\lambda_1}+2\sqrt{\lambda_2})}(-1+e^{\eta\sqrt{\lambda_1}})(-1+e^{\eta_\infty\sqrt{\lambda_1}})(-e^{\eta\sqrt{\lambda_1}}+e^{\eta_\infty\sqrt{\lambda_1}})(-1+e^{2\eta_\infty\sqrt{\lambda_2}})\lambda_2\lambda_3$$
$$+ 2\lambda_1(-2e^{(2\eta+\eta_\infty)(\sqrt{\lambda_1}+\sqrt{\lambda_2})}\sinh((\eta-\eta_\infty)\sqrt{\lambda_1})\sinh(\eta_\infty\sqrt{\lambda_2})\lambda_2(c_3-\lambda_1+\lambda_2)$$
$$- c_3e^{(2\eta+\eta_\infty)\sqrt{\lambda_2}}(e^{2\eta\sqrt{\lambda_1}}-e^{2(\eta+\eta_\infty)\sqrt{\lambda_1}})(\sinh((\eta-\eta_\infty)\sqrt{\lambda_2})\lambda_2$$
$$- (-\sinh(\eta\sqrt{\lambda_2})+\sinh((\eta-\eta_\infty)\sqrt{\lambda_2})+\sinh(\eta_\infty\sqrt{\lambda_2}))\lambda_3))))),$$

$$f''(\eta) = \frac{1}{2\sqrt{\lambda_1}(\lambda_1-\lambda_2)\sqrt{\lambda_2}}(e^{-2\eta(\sqrt{\lambda_1}+\sqrt{\lambda_2})}(-1+\coth(\eta_\infty\sqrt{\lambda_1}))(-1+\coth(\eta_\infty\sqrt{\lambda_2}))$$
$$\cdot (2e^{(2\eta+\eta_\infty)(\sqrt{\lambda_1}+\sqrt{\lambda_2})}\sinh(\eta_\infty\sqrt{\lambda_2})\sqrt{\lambda_2}(\cosh((\eta-\eta_\infty)\sqrt{\lambda_1})\lambda_1(c_3-\lambda_1+\lambda_2)$$
$$+ c_3(\cosh(\eta\sqrt{\lambda_1})-\cosh((\eta-\eta_\infty)\sqrt{\lambda_1}))\lambda_3)+c_3e^{(2\eta+\eta_\infty)\sqrt{\lambda_2}}(e^{2\eta\sqrt{\lambda_1}}-e^{2(\eta+\eta_\infty)\sqrt{\lambda_1}})\sqrt{\lambda_1}$$
$$\cdot (\cosh((\eta-\eta_\infty)\sqrt{\lambda_2})(\lambda_2-\lambda_3)+\cosh(\eta\sqrt{\lambda_2})\lambda_3))),$$

$$f''(0) = \frac{1}{2\sqrt{\lambda_1}(\lambda_1-\lambda_2)\sqrt{\lambda_2}}((-1+\coth(\eta_\infty\sqrt{\lambda_1}))(-1+\coth(\eta_\infty\sqrt{\lambda_2}))$$
$$\cdot (c_3e^{\eta_\infty\sqrt{\lambda_2}}(1-e^{2\eta_\infty}\sqrt{\lambda_1})\sqrt{\lambda_1}(\cosh(\eta_\infty\sqrt{\lambda_2})(\lambda_2-\lambda_3)+\lambda_3)$$
$$+ 2e^{\eta_\infty(\sqrt{\lambda_1}+\sqrt{\lambda_2})}\sinh(\eta_\infty\sqrt{\lambda_2})\sqrt{\lambda_2}(\cosh(\eta_\infty\sqrt{\lambda_1})\lambda_1(c_3-\lambda_1+\lambda_2)$$
$$- c_3(-1+\cosh(\eta_\infty\sqrt{\lambda_1}))\lambda_3))),$$

$$\theta(\eta) = \frac{1}{2\lambda_2}\Big(e^{-\eta\sqrt{\lambda_2}}\Big((-e^{2\eta\sqrt{\lambda_2}}+e^{2\eta_\infty\sqrt{\lambda_2}})(-1+\cosh(\eta_\infty\sqrt{\lambda_2}))\lambda_2$$
$$+ 2\Big(-1+e^{\eta\sqrt{\lambda_2}}+\frac{1-e^{2\eta\sqrt{\lambda_2}}}{1+e^{\eta_\infty\sqrt{\lambda_2}}}\Big)\lambda_3\Big)\Big),$$

$$\theta'(\eta) = \frac{\operatorname{csch}(\eta_\infty\sqrt{\lambda_2})(-\cosh(\eta\sqrt{\lambda_2})\lambda_3+\cosh((\eta-\eta_\infty)\sqrt{\lambda_2})(-\lambda_2+\lambda_3))}{\sqrt{\lambda_2}},$$

$$\theta'(0) = \frac{\operatorname{csch}(\eta_\infty\sqrt{\lambda_2})(-\cosh(x\sqrt{\lambda_2})\lambda_3+\cosh((x-\eta_\infty)\sqrt{\lambda_2})(-\lambda_2+\lambda_3))}{\sqrt{\lambda_2}}.$$